ACS OMEGA

Article

Cite This: ACS Omega 2017, 2, 8156-8166

http://pubs.acs.org/journal/acsodf

Fluorescent and Photosensitizing Conjugates of Cell-Penetrating Peptide TAT(47-57): Design, Microwave-Assisted Synthesis at 60 °C, and Properties

Nancy M. Okuda-Shinagawa,[†] Yulia E. Moskalenko,[†] Helena C. Junqueira,[†] Maurício S. Baptista,[†] Carlos M. Marques,[‡,†] and M. Terêsa Machini*[,†]

[†]Department of Biochemistry, Institute of Chemistry, University of São Paulo, Av. Prof. Lineu Prestes, 748, Cidade Universitária, Butantã, 05508-000 São Paulo, SP, Brazil

[‡]Institut Charles Sadron, Université de Strasbourg, UPR22-CNRS, 23, rue du Loess, BP 84047, 67034 Strasbourg Cedex 2, Strasbourg, France

Supporting Information

ABSTRACT: Conjugates based on cell-penetrating peptides (CPPs) are scientifically relevant owing to their structural complexity; their ability to enter cells and deliver drugs, labels, antioxidants, bioactive compounds, or DNA fragments; and, consequently, their potential for application in research and biomedicine. In this study, carboxyamidated fluorescently labeled conjugates FAM-GG-TAT(47-57)-NH_2 and FAM-PEG_6-TAT(47-57)-NH_2 and photosensitizer-labeled conjugate Ch_k-PEG_6-TAT(47-57)-NH_2 [where TAT(47-57) is the CPP, 5(6)-carboxyfluorescein is the (FAM) fluorophore, chlorin k (Ch_k) is the photosensitizer, and the dipeptide glycyl−glycine (GG) or hexaethylene glycol (PEG_6) is the spacer] were originally designed, prepared, and fully characterized. Practically, all chemical reactions of the synthetic steps (peptide synthesis, spacer incorporation, and conjugation) were microwave-assisted at 60 °C using optimized protocols to give satisfying yields and high-quality products. Detailed analyses of the conjugates using spectrofluorimetry and singlet oxygen detection showed that they display photophysical properties typical of FAM or Ch_k. Anticandidal activity assays showed that not only this basic property of TAT(47-57) was preserved in the conjugates but also that the minimal inhibitory concentration was slightly reduced for cells incubated with PS-bearing conjugate Ch_k-PEG_6-TAT(47-57)-NH_2. Overall, these results indicated that the synthetic approach on-resin assisted by microwaves at 60 °C is simple, straightforward, selective, metal-free, sufficiently fast, cleaner, and more cost-effective than those previously used for preparing this type of macromolecule. Furthermore, such new data show that microwaves at 60 °C and/or conjugation did not harm the integrity of the conjugates' constituents. Therefore, FAM-GG-TAT(47-57)-NH_2, FAM-PEG_6-TAT(47-57)-NH_2, and Ch_k-PEG_6-TAT(47-57)-NH_2 have high potential for practical applications in biochemistry, biophysics, and therapeutics.

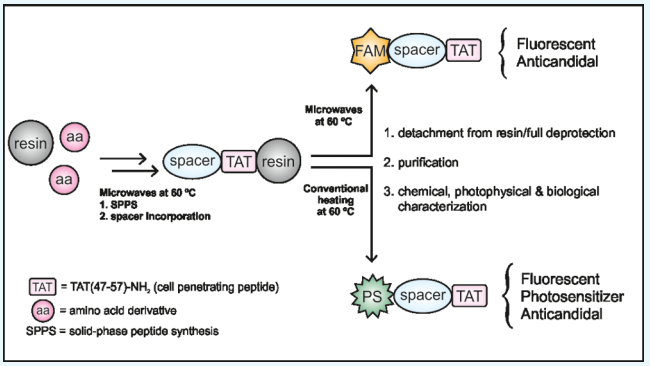

INTRODUCTION

Chemical compounds with the ability to enter cells or specifically affect them are the front-runners in the quest to fight diseases. Hence, there is a growing interest in the chemistry and structure of cell-penetrating or cell-modifying agents as well as in the fundamental mechanisms by which they interact with cellular membranes and their model counterparts, the lipid membranes.

Cell-penetrating peptides[1] (CPPs) are short amino acid sequences[2] able to enter different cells;[3−5] thus, they have been named "biological Trojan horses"[6] and have been employed in cellular delivery of cargoes such as DNA,[7] siRNA,[8] organic halide,[9] ruthenium complex,[10] ^{89}Zr-labeled antibody for PET imaging,[11] low-molecular-weight chitosan,[12] and fluorescent dyes.[13] This strategic property has also increased the interest on CPP interaction with biological membranes (BMs) and their uptake pathways[14] as well as has aided understanding BM properties. Because BMs are very complex supramolecular fluids, simplified models or biomimetic membranes (BMMs)[15−17] have frequently replaced them in biophysical studies. In fact, studies with BMMs have also helped investigating cell internalization mechanisms. A good example is the work of Dennison et al., who found out that penetration is affected when hydrophobic molecules are attached to TAT.[18]

Among the hundreds of CPPs identified so far,[19] TAT peptides are perhaps the most studied and found in practical uses. TAT peptides are fragments of the human immunodeficiency virus 1 protein containing 86−102 amino acid residues

Received: August 3, 2017
Accepted: October 30, 2017
Published: November 20, 2017

DOI: 10.1021/acsomega.7b01127
ACS Omega 2017, 2, 8156−8166

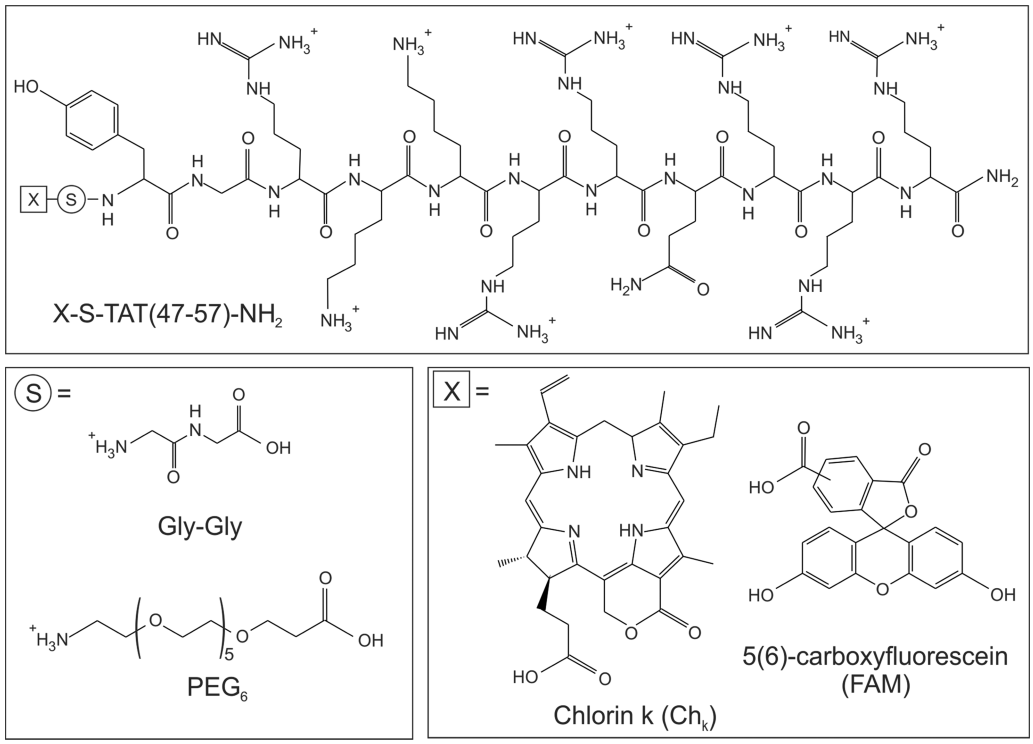

Figure 1. Protonated structures of the conjugates synthesized in this work and of their building blocks.

and exhibiting three domains responsible for transactivation, DNA binding, and nuclear transport,[14] one of them being the arginine-rich basic domain 48−60 (GRKKRRQRRRPPQ).[20] TAT(47-57), YGRKKRRQRRR,[21] is frequently employed for covalent binding to peptides, proteins, fluorophores,[22] chelators,[23] and DNA,[7] with the aim of delivering them to different cells through translocation across their plasma membranes. Such examples illustrate the high interest in TAT(47-57)-based conjugates in research and biomedicine. In the last case, the following information speaks for itself: in 2015, Fosgerau and Hoffmann stated that 140 peptide drugs were in clinical trials and more than 500 therapeutic peptides in preclinical tests;[24] this year, Lau and Dunn are reporting: "over 60 peptide drugs have been approved in the United States, Europe, and Japan; over 150 are in active clinical development, and an additional 260 have been tested in human clinical trials".[25]

Selective covalent binding between a CPP and a cargo to produce a conjugate involves consideration of their chemically reactive groups and structural properties, selection of a suitable synthetic approach, and establishment of conditions. Most studies on TAT peptide-based conjugates containing the cargo covalently bound to the CPP have employed (i) traditional solid-phase synthesis (in which all reactions are performed at room temperature), (ii) exposure of the resultant fully protected CPP to acidic conditions for the release of the crude unprotected TAT, and (iii) conjugation in solution.[20,22,26−30] In fact, up to 2014, the on-resin method seemed to be less used than the in-solution method for the conjugation of variable cargoes with TAT or linker-TAT prepared on-resin. Among the conjugates prepared, some have a spacer between the TAT peptide and the cargo, such as a disulfide carbonate linker,[30] PEG_6,[31,32] or an amino acid side chain,[20] but others have the cargo molecule directly connected to the terminal amino acid.[28] Conjugates DFO-Suc-TAT(47-57), DFX-TAT-(47-57), and DFO-Suc-TAT(49-57), where Suc was succinic acid and DFO and DFX were desferrioxamine and deferasirox, respectively, are examples of spacer-containing TAT-based conjugates fully synthesized on-resin[23,33,34] as the conjugation of DFO-Suc occurred at the N-terminus of the TAT peptide-resin, a highly selective approach carried out traditionally (at room temperature) or at 60 °C using conventional heating.

The present study is a step forward for the chemistry and development of CPP-based conjugates as it originally encompasses (i) the design of new potentially useful carboxyamidated TAT-based conjugates; (ii) their on-resin syntheses assisted by microwaves at 60 °C using optimized protocols; (iii) chemical, photophysical, and biological analyses of the conjugates to verify if conjugation and/or microwaves at 60 °C had any impact on the typical properties of the conjugate constituents. Indeed, despite having structural similarity with conjugated variants of TAT(47-57) previously reported, FAM-GG-TAT(47-57)-NH_2, FAM-PEG_6-TAT(47-57)-NH_2, and Ch_k-PEG_6-TAT(47-57)-NH_2 [where TAT(47-57): CPP, FAM: fluorophore 5(6)-carboxyfluorescein, Ch_k: photosensitizer chlorin k, GG: glycyl−glycine, and PEG_6: hexaethylene glycol] have never been reported. Additionally, (i) the photosensitizer Ch_k has not been conjugated with a peptide and (ii) although solid-phase synthesis has been used to make this type of conjugate, very few employed microwaves for the synthesis of TAT(47-57) or TAT(47-57)-NH_2 and no one used microwaves at 60 °C with the protocols that we have been establishing and appraising. Moreover, detailed analysis of the conjugates to assess if they displayed typical properties of their constituents (and, therefore, if the synthetic approach used is suitable for the synthesis of such macromolecules) is unique.

The motivations for using fluorophore FAM and photosensitizer Ch_k as TAT(47-57)-NH_2 cargoes were the following:

(a) 5-Carboxyfluorescein and 6-carboxyfluorescein (5-FAM and 6-FAM, respectively) display fluorescent properties

DOI: 10.1021/acsomega.7b01127
ACS Omega 2017, 2, 8156−8166

Scheme 1. (i) Fmoc-Gly-OH (2.5 equiv), HOBt (2.5 equiv), DIC (2.5 equiv), DMF, 20 min, 60 °C; (ii) Fmoc-NH-PEG_6-COOH (2.5 equiv), HATU (2.5 equiv), DIPEA (5 equiv), DMF, 2 × 30 min, 60 °C; (iii) 25% 4-methyl-piperidine/DMF, 5 min, 60 °C; (iv) FAM (5 equiv), BOP (5 equiv), HOBt (5 equiv), DIPEA (15 equiv), DMF, 2 × 30 min, 60 °C; (v) chlorin k (2.5 equiv), HOBt (2.5 equiv), HATU (2.5 equiv), DIPEA (7.5 equiv), DMF, 14.5 h, 60 °C, 300 rpm; (vi) TFA/scavengers, 2 h, 60 °C, 300 rpm

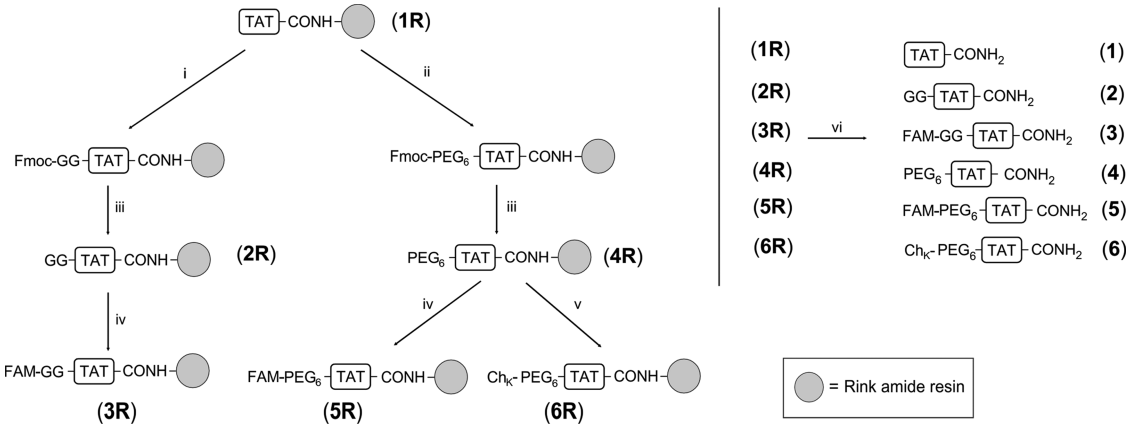

with absorption at 492 nm and emission at 518 and 515 nm, respectively.[35] Because of the high cost and difficulty to separate them, the two isomers are commercially available and used as a mixture commonly abbreviated as FAM.[36,37] FAM is probably the most popular fluorescent dye used for labeling and imaging applications[35] involving peptides,[38−40] proteins,[41] and oligonucleotides.[36] FAM-labeled peptides and proteins have been widely used to understand their interactions with BMs[39,42,43] or BMMs.[44,45]

(b) a PS is a molecule singlet in its ground state that, when exposed to appropriate quantum energy, goes to an unstable singlet excited-state and loses its energy excess either by light emission (fluorescence) or heat production (internal conversion).[46] When the PS excited state undergoes electron/energy transfer reactions, several oxidant species (including $^1O_2$) are generated.[47] These photochemical processes have been intentionally used to kill/induce death and destroy targeted cells and/or tissues in photodynamic therapy (PDT),[48] where a PS is administered and activated by light in a specific wavelength.[49] To overcome their low selectivity[50] and hydrophobicity,[51] the PSs have been conjugated to saccharides,[52] proteins,[53] antibodies,[54] polymers,[55] and peptides,[50] including CPPs.[56−58]

RESULTS AND DISCUSSION

Design of New CPP-Based Conjugates. Figure 1 shows the chemical structures of the building blocks of the target conjugates. Either the properties of the CPP TAT(47-57), FAM, and Ch_K cited above or the following information served as background for their design:

1. Peptide carboxyamidation certainly would help obtaining TAT(47-57)-based conjugates chemically more stable in physiological media because carboxypeptidases would not act on them.
2. Glycyl−glycine (12 atoms) and PEG_6 (21 atoms) could act as spacers for coupling of FAM or Ch_k to **1R** (Scheme 1) as they could minimize steric hindrance between the bulky fluorescent and phototherapeutic cargo and, consequently, help preserving the photophysical properties of such building blocks. In addition, the spacers' polar nature was expected to increase water solubility of the conjugates.[59] Furthermore, they are chemically and biologically inert. Indeed, PEGs of low molecular masses are also reported to display low cytotoxicity; thus, PEG_6 would not significantly interfere in potential cell toxicity displayed by intermediate PEG_6-TAT(47-57)-NH_2 and by conjugates FAM-PEG_6-TAT-(47-57)-NH_2 and Ch_k-PEG_6-TAT(47-57)-NH_2.
3. Although the antimicrobial peptides (AMPs) have the ability to kill bacteria and fungi by disrupting their plasma membrane or affecting a specific intracellular target,[60] PSs can do the same by inducing oxidative stress at multiple cellular targets. Therefore, it is not surprising that conjugates of PS-AMPs have been assembled and examined on their potential for use in antimicrobial photodynamic therapy (PDT).[61]

Synthesis of the TAT(47-57)-Based Conjugates. In the present study, we projected that the synthesis of the designed conjugates would be even faster and relatively more environmentally friendly if experimental conditions very similar to those established by us for manual peptide solid-phase synthesis at 60 °C using conventional heating,[62,63] recently used for making iron-chelating TAT conjugates,[34] were adapted for the new compounds and for conduction on the CEM equipment under N_2 stirring and microwave irradiation at 60 °C. It is essential to highlight that the protocols employed are somewhat different from those often used for microwave-assisted solid-phase peptide synthesis as our couplings and deprotections are not as fast as those regularly described,[64,65] but they have been proven to minimize amino acid enantiomerization,[62] a critical aspect to be considered when high temperature and microwaves are used in synthetic chemistry of peptide and peptide-based compounds.

Scheme 1 summarizes all steps of the synthetic route. Each chemical reaction was monitored by the Kaiser test[66] of the corresponding resin, peptidyl-resin (**1R**), spacer-peptide-resin (**2R** and **4R**), or conjugate-resin (**3R**, **5R**, and **6R**) beads.

Step 1: Microwave-Assisted Solid-Phase Peptide Synthesis of 1R. TAT(47-57) was assembled on-resin to obtain peptidyl-resin **1R**, which was divided into three parts for the preparation

DOI: 10.1021/acsomega.7b01127
ACS Omega 2017, 2, 8156−8166

Table 1. Purification by RP-HPLC and Analytical Data of the Purified Target Compounds

compound (Scheme 1)	purification yield (%)	purity degree (%)	peptide content (%)	molar mass	ESI-MS of **1**–**6**		
					m/z; $z = 1$ expected	base peak observed (m/z; $z = 3$)	corresponding ion (calculated m/z; $z = 3$)
1	62	99	56.7	1558.90	1559.90	634.50	634.63 ($M + 3TFA^-$)
2	59	98	58.5	1672.98	1673.98	672.50	672.66 ($M + 3TFA^-$)
3	35	100	51.6	2031.29	2032.29	754.10	754.10 ($M + 2TFA^-$)
4	39	100	59.5	1894.30	1895.30	560.10[b]	560.08[b] ($M + 3TFA^-$)
5	33	100	70.9	2252.59	2253.59	827.80	827.86 ($M + 2TFA^-$)
6	[a]	69	70.1	2426.95	2427.95	923.98	923.98 ($M + 3TFA^-$)

[a]Because of the very little amount prepared and its acceptable purity degree, this conjugate was not further purified by RP-HPLC. [b]m/z, $z = 4$. TFA^- = trifluoroacetate counterion.

of the target conjugates. To our knowledge, this is the first report on the synthesis of this TAT peptide using the approach and protocols described here. Confirming our previous studies on microwave-assisted SPPS at 60 °C,[62,63] this combination was efficient and shortened the assembling of **1R** in comparison to that performed earlier using traditional SPPS[23,33] or SPPS at 60 °C using conventional heating.[34] In fact, under the conditions used, the Fmoc-removal reactions were accomplished within 5 min and the acylation reactions were completed within 20 min, except for the acylation of the growing peptidyl-resin by Fmoc-Arg[7](Pmc)-OH that had to be repeated for completion. Peptide cleavage from resin/full deprotection of about 10 mg of **1R** gave crude product **1** containing the desired amidated TAT(47-57) as the major component, as shown by RP-HPLC (conditions in Table S1) and LC/ESI-MS (Figures S1 and S2 of Supporting Information).

*Step 2: Introduction of Spacer Gly-Gly or PEG_6 into **1R** To Obtain **2R** or **4R**, Respectively.* Two subsequent acylations of **1R** by Fmoc-Gly-OH followed by Fmoc removals were done with microwaves at 60 °C using optimized protocols and HOBt/DIC for carboxyl group activation.[62] Peptide-resin weight gain (13 mg) and analysis by LC-ESI/MS (LC conditions in Table S1) of crude product **2** obtained from peptide cleavage/full deprotection of **2R** (about 10 mg) indicated that (i) the dipeptide was successfully incorporated into the fully protected CPP-resin and (ii) despite the microwaves and high temperature used, such incorporation occurred with very low extension of Fmoc removal from acylating reagent Fmoc-Gly-OH and/or its active ester (**2R**) formed in the reaction medium.[39,63,67]

Likewise, and under similar conditions using HATU/DIPEA for carboxyl activation,[68,69] two reactions of 30 min were needed for the total attachment of the PEG_6 spacer to **1R**, which was confirmed by resin weight gain (10 mg) and analysis by LC-ESI/MS (LC conditions in Table S1) of crude product **4** obtained from peptide cleavage/full deprotection of a small sample of **4R** (10 mg). This result is in agreement with previous attempts to incorporate PEG_6 to a peptidyl-resin.[68]

*Step 3: Attachment of FAM to **2R** and **4R** To Produce **3R** and **5R**, Respectively.* The coupling reaction was also carried out on-resin with microwaves at 60 °C using optimized protocols and BOP/HOBt/DIPEA for carboxyl activation.[39,42] Monitoring by the Kaiser test showed that the reaction starting from **4R** was faster than that starting from **2R**: indeed, to be completed, the first required 60 min (2 × 30 min) and the second demanded 90 min (3 × 30 min). Because the same molar excess of FAM was used and knowing that this is a bulky compound (Figure 1), these results revealed that the size and nature of the spacer play a decisive role in the incorporation of the cargo molecule into the spacer-CPP-resin. In addition, they suggest that such attachment would be sluggish if carried out at room temperature and/or were not assisted by microwaves. Weight gains of **2R** and **4R** (7 and 10 mg, respectively) and analyses by LC-ESI/MS of crude products **3** and **5** (LC conditions in Table S1) resulting from peptide cleavages/full deprotections of small samples of **3R** and **5R** (about 10 mg of each) indicated that the target conjugates were finally obtained.

*Step 4: Attachment of Ch_k to **4R** Aiming at Obtaining **6R**.* Inspired by a previous work,[70] the coupling reaction was performed under orbital shaking at 60 °C for 14 h using HATU/HOBt/DIPEA and our customized protocols for acylation of peptide-resins. In this case, the reaction was not microwave-assisted because, due to limitation of Ch_k, the volume of the reaction media (1.5 mL) did not reach the minimum volume (3 mL) required for the oven/apparatus employed. Again, the weight gain of **4R** and analytical data (LC conditions in Table S1) of crude product **6** confirmed that the coupling was completed to give the desired conjugate **6** as the major component.

*Steps 5–7: Conjugate Detachment from the Resin/Full Deprotection on Semipreparative Scale, Purification of the Crudes, and Characterization of Purified Compounds **1**–**5**.* Analysis by RP-HPLC and LC-ESI-MS of the crudes obtained gave exactly the same results found for those obtained on analytical scale (Figures S1 and S2 of Supporting Information); thus, conditions for purification by RP-HPLC were established (Table S1), except for conjugate **6** used in its crude form. The RP-HPLC profiles and mass spectra of the final compounds allowed the evaluation of their purity degrees and confirmed their identities. Table 1 describes the purification yields as well as the purity degrees and peptide contents of purified compounds **1**–**6**. As expected, because the synthetic arginine-rich peptide conjugates are cationic and were purified using a TFA-based solvent system, they contain trifluoroacetate (TFA^-) counter ions, which explains the ions of higher mass/charge ratios (m/z) detected and listed in the same table. Such a statement was confirmed with the help of RP-HPLC of purified TAT(47-57)-NH_2 using a formic acid-based solvent system to swap the TFA^- followed by Direct Infusion Mass Spectrometry analysis of the eluted peptide (data not shown). Detailed results are shown in the Supporting Information.

Altogether, the results above demonstrated that the combination of SPPS and microwave irradiation at 60 °C using optimized protocols was extremely beneficial for the total synthesis of the target macromolecules. Positively, the microwave-assisted on-resin steps at 60 °C (aminoacylations of the resin or peptide assembly, Fmoc deprotections, and acylation of

DOI: 10.1021/acsomega.7b01127
ACS Omega 2017, 2, 8156–8166

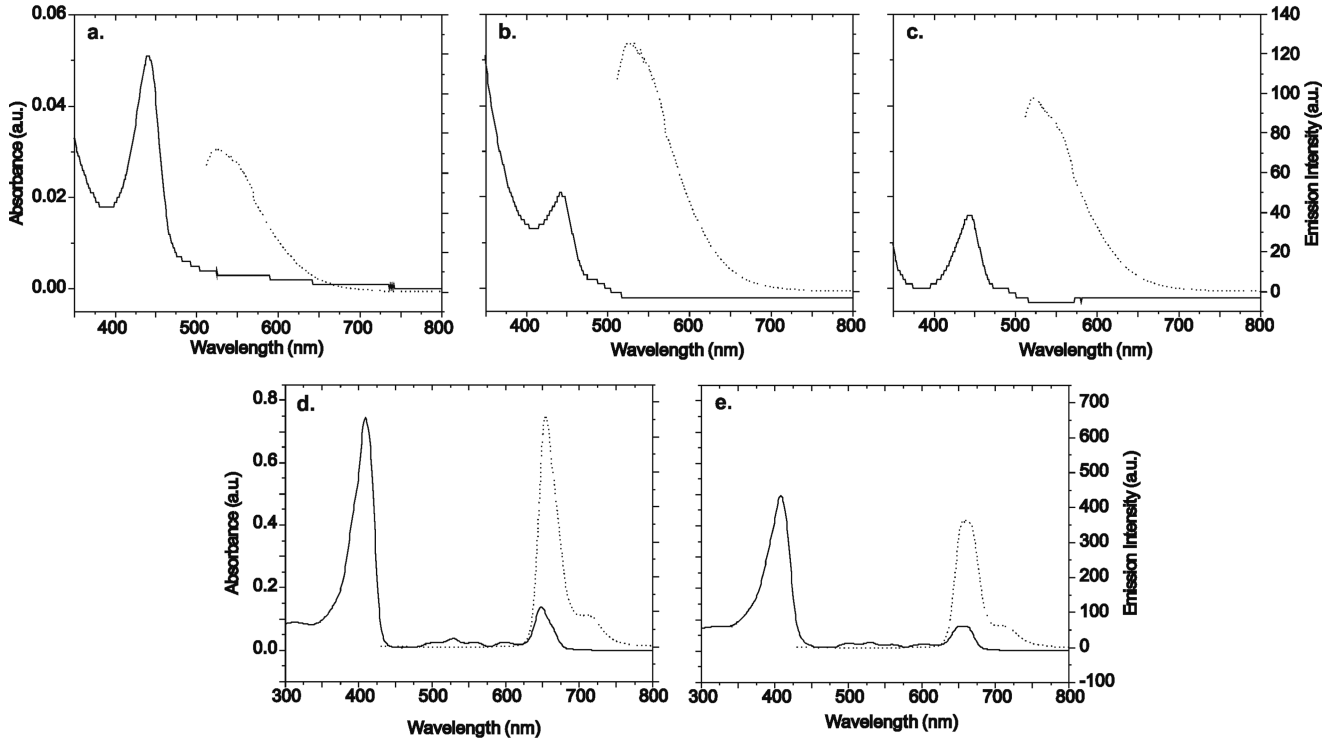

Figure 2. Absorbance (left axis; solid line) and emission (right axis; dashed line) spectra of (a) FAM, (b) conjugate **3**, (c) conjugate **5**, (d) chlorin k, and (e) conjugate **6** at the same concentration.

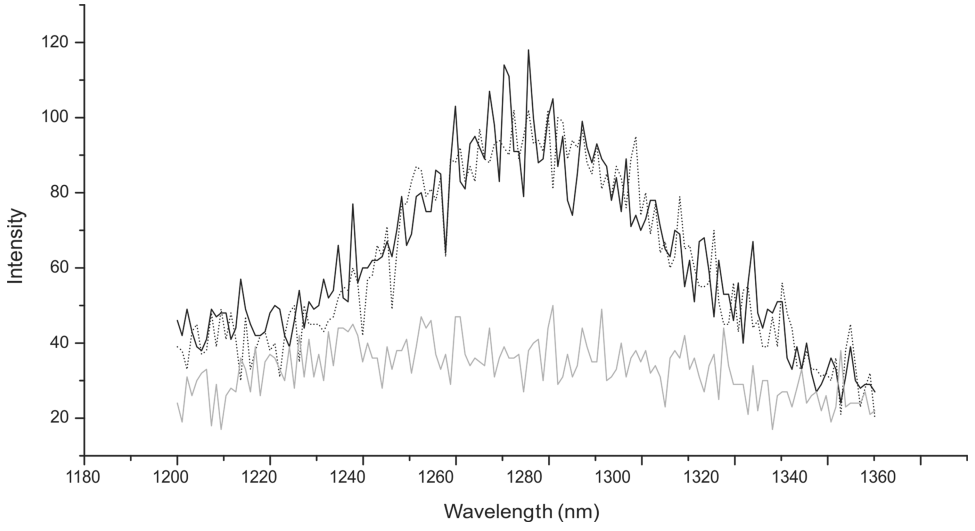

Figure 3. Photosensitized singlet oxygen generation and detection for free Ch_k (solid black line), conjugate **4** (solid gray line), or conjugate **6** (dotted line).

the CPP-resin by FAM or PEG_6) occurred with reasonable yields and were sufficiently fast, selective, metal-free, reasonably priced, and, also, relatively clean. These features satisfy the increasing worldwide demand for faster, more selective, and cleaner means to prepare fine chemicals of high quality with satisfactory yields. Additionally, the high speed and cost-effectiveness of the synthetic approach used in the present study are especially important features if B. Merrifield's statement in his Nobel lecture (1984) is considered: "...When a multistep process, such as the preparation of a long polypeptide or protein, is contemplated, the saving in time and effort and materials could be very large...".

Photophysical Properties of the Purified Synthetic Conjugates. Because conjugates **3**, **5**, and **6** were fully or mostly synthesized under microwave irradiation at 60 °C expecting to obtain new conjugates with potential for practical uses, chemical characterization (for identity confirmation and, consequently, demonstration of structural integrity) and examination of the basic properties of their constituents (light absorption, fluorescence emission and/or photodegradation, antimicrobial activity with and without illumination) were conducted, using FAM and Ch_K as references. Altogether, the results indicated that we succeeded in our endeavor as the conjugates obtained were the desired ones with the desired properties.

DOI: 10.1021/acsomega.7b01127
ACS Omega 2017, 2, 8156−8166

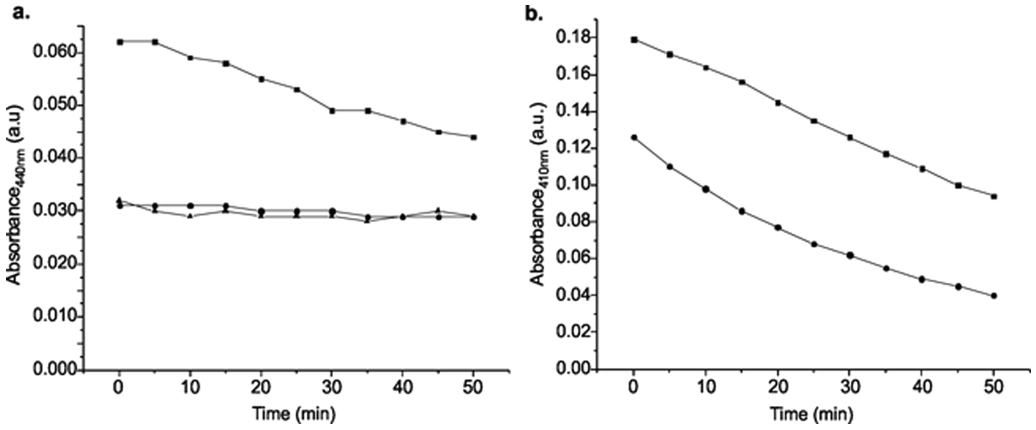

Figure 4. Photodegradation curves of (a). FAM (■), conjugate 3 (●), and conjugate 5 (▲) and of (b). chlorin k (■) and conjugate 6 (●) at the same concentration.

Figure 2 shows the light absorption and fluorescence emission spectra of all compounds at equivalent concentration. The similarity of profiles (presence of identical bands) in Figure 2a–c indicated that FAM's photophysical properties were preserved in the conjugates, meaning that microwaves at 60 °C and/or incorporation of any of the two spacers followed by conjugation were harmless. The significantly lower intensities of the band at 440 nm in Figure 2b,c (for FAM-containing conjugates **3** and **5**) in comparison to those in Figure 2a (for free FAM) are probably explained by the existence in **3** and **5** of a covalent bond between the fluorophore and spacer-TAT(49-57)-NH_2. This hypothesis finds support in similar observations made by Li et al. when comparing the photophysical properties of FAM-containing peptides with those of free FAM.[40] Conversely, the fluorescence signals in the spectra of **3** and **5** were not drastically reduced: actually, a little positive effect was observed in b and c, indicating that the conjugation did not create any channel of nonradiative deactivation of the excited singlet state. It appears that this is the first work to use spacer Gly-Gly or PEG_6 for the conjugation of this fluorophore to TAT(47-57) and to demonstrate whether FAM's properties were preserved. Indeed, for instance, in previous works, FAM was directly linked to the N-terminal of the peptide-resin[71−73] or to a C-terminal linked by a Lys[44] or, yet, used as a modified FAM (carboxyfluorescein succinimidyl ester).[45]

With respect to the spectra recorded for Ch_k and Ch_k-containing conjugate **6**, they were also very similar (Figure 2d,e), indicating preservation of photophysical properties of the PS after conjugation. As described above, either the intensities of the two bands at 400 and 650 nm or the fluorescence of the conjugate was partly reduced.

Experiments of singlet oxygen detection were carried with Ch_k, conjugate **4**, and conjugate **6** in 60% acetonitrile (ACN)/0.09% TFA in H_2O to compare their chemical stabilities and consequent preservation of the phototherapeutic (singlet oxygen generation) properties of the PS even when covalently bound to the PEG_6-TAT peptide (**4**). Reading scans at 1200–1360 nm obtained after exposure of their solutions to a laser at 410 nm demonstrated that **4** provided a low-intensity $^1O_2$ signal, but Ch_k and Ch_k-containing conjugate **6** presented equivalent high-intensity signals (Figure 3), meaning that the conjugation did not influence this photosensitizer property. The $^1O_2$ lifetimes measured in the solvent used were 13.4 μs for Ch_k and 13.7 μs for conjugate **6**, which are very similar to the lifetime value reported previously for 50% ACN in H_2O (15–22 μs).[74]

The photostabilities of the conjugates synthesized **3**, **5**, and **6** were also examined by laser irradiation of their solutions at identical concentrations, followed by registration of their UV/vis absorption spectra every 5 min for 50 min. The photodegradation curves of FAM and its conjugates (**3** and **5**) at 440 nm are shown in Figure 4a. As observed, the absolute value of absorbance is smaller for the conjugate. However, whereas absorbance readings for FAM varied from 0.062 to 0.040 (difference of 0.022) in 50 min of exposure to light, absorbances for conjugates **3** and **5** were considerably stable (varying from 0.031 to 0.029; difference of 0.003). Therefore, it is possible to uphold that photodegradation was not as prominent for the conjugate as for the free FAM.

Figure 4b shows the decay curves obtained for Ch_k and for Ch_k-containing conjugate **6** at 410 nm. Despite the difference of intensity, the pattern is definitely the same, clearing any possible effect of the conjugation on such specific Ch_k's property. These results are also supported by a previous study focused on conjugates composed by porphyrins bound to a cationic antimicrobial peptide[61] as discussed below.

Antimicrobial and Cell-Penetrating Activity of the Purified Synthetic Conjugates. Knowing that TAT peptide (47-58), a carboxyl-free analogue of TAT(47-57)-NH_2 used as CPP in the present study, has the ability to inhibit the growth of bacteria and *Candida albicans* cells (AMP activity) without hemolytic effect on human erythrocytes, penetrate, and localize in the nucleus of HeLa and *Trichosporon beigelii* cells (CPP activity),[75,76] liquid growth inhibition assays were performed to verify whether the new conjugates also presented anticandidal activity. Compounds **1**, **2**, and **4** were used as controls. *Candida parapsilosis* was chosen as the target microorganism because likewise *C. albicans* it is involved in infections of major clinical importance. In addition, its significance and prevalence has been dramatically increased.[77]

Table 2 describes the minimal inhibitory concentrations (MICs) found. Those of conjugates **3**, **5**, and **6** revealed that the synthetic approach used, the incorporation of a spacer followed by covalent binding of FAM or Ch_k, did not extinguish the antimicrobial activity displayed by compound **1**, the building block TAT(47-57)-NH_2. On the other hand, the slightly higher MIC observed for conjugate **5** could suggest that either the nature of the cargo or the length of the spacer may have an impact on the bioactivities of TAT-based conjugates

DOI: 10.1021/acsomega.7b01127
ACS Omega 2017, 2, 8156–8166

Table 2. MIC Values for the Anticandidal Assay against *C. parapsilosis*, ATCC 22019

compound	MIC values[a] (μmol·L^{-1})	
	dark	light irradiation[b]
1	12.5	[c]
2	12.5	[c]
3	12.5	[c]
4	12.5	[c]
5	25.0	[c]
6	12.5	6.25

[a]Average resulting from triplicates. [b]By led array (408 nm) for 40 min, to have a total light dose of 10 J·cm^{-2}. [c]Not measured.

(indeed, conjugate **5** has FAM as cargo instead of Ch_k present in conjugate **6**; conjugate **3** contains a GG as a spacer instead of PEG_6 present in conjugate **5**). Anyway, the overall results were very satisfying because they reinforced that each building block of the conjugates reported here had its basic properties preserved. Although the MICs found are higher than those usually reported for antibiotics,[77] they are at the concentration range often found for antimicrobial peptides and CPPs with antimicrobial activities,[78−80] including TAT(47-57),[76] as well as they are consistent with the contemporary literature in which labeling of AMPs and/or CPPs with FAM has been explored to better investigate by fluorescence microscopies their mode of action on microbes;[39,42] their interactions with BMs,[39] BMMs, or intracellular targets; and drug delivery. Thus, no further experiment in this direction seemed to be required in the present study. Overall, such results support the idea that the new conjugates have potential for practical applications.

Because conjugate **6** contains a PS as a cargo molecule covalently bound to a CPP with anticandidal activity (thus being an antifungal cationic PS), assay against *C. parapsilosis* cells was also carried out with irradiation by a led array at 408 nm. As predicted, light irradiation slightly increased the yeast susceptibility, which was strongly suggestive of conjugate **6** cell internalization: in fact, cell penetration and light irradiation may have allowed the Ch_k present in its structure to cause oxidative stress, potentiating the anticandidal activity observed in the dark.

CONCLUSIONS

We have designed, synthesized, and characterized original TAT(47-57)-based conjugates that can find practical uses owing to their photophysical properties, anticandidal activity, and high potential to enter the nucleus of bacterial, fungal, and human cells. To our knowledge, this is the first study to either conjugate Ch_k to a peptide or employ microwave irradiation at 60 °C for solid-phase synthesis of TAT(47-57)-based conjugates (peptide synthesis, incorporation of a spacer, and conjugation). Some features of the synthetic approach and protocols employed are in agreement with the principles of green chemistry.

EXPERIMENTAL SECTION

Synthesis of Cell-Penetrating Peptide-Resin (1R). TAT(47-57) was manually assembled on a solid support (**S**olid-**P**hase **P**eptide **S**ynthesis; SPPS) using 9-**F**luorenyl**m**e-th**o**xy**c**arbonyl (Fmoc) chemistry using protocols established in our laboratory for microwave-assisted SPPS at 60 °C,[62,81] which were adapted to the target compounds. Fmoc-Arg(Pmc)-OH, Fmoc-Gln-OH, Fmoc-Lys(Boc)-OH, Fmoc-Gly-OH, and Fmoc-Tyr(tBu)-OH were used as acylating reagents, purchased from Bachem, NovaBiochem-Merck (Germany), or ChemPep. The reactions (couplings) and Fmoc removal (deprotections) required for peptide chain assembly on-resin were carried out in a 25 mL polypropylene vessel placed into the microwave cavity of the 300 W single-mode manual microwave peptide synthesizer (CEM, Discover SPS) using 60 °C as the setup temperature. Although power pulsing sequences of 5 W for 20 min were used for coupling steps (2.5 equiv of Fmoc-amino acid, 2.5 equiv of *N*,*N*′-diisopropylcarbodiimide (DIC), 2.5 equiv of 1-hydroxybenzotriazole (HOBt), and 1 equiv of the resin or the peptide-resin in DMF), 20 W for 5 min were used for deprotections (25% 4-methyl-piperidine in DMF). Reactions were stirred by N_2 bubbling, and their temperatures were monitored continuously with a fiber optic probe inserted into the reaction vessel; the volumes varied from 13.0 to 15.0 mL. To obtain a C-terminal C(O)-NH_2 using 4-(2′,4′-dimethoxyphenyl-Fmoc-aminomethyl)phenoxy, resin of 0.3 mmol/g substitution degree (Rink amide, Bachem) was employed. Coupling and deprotection reactions were followed by alternate washing with DMF, MeOH, and 25% DMSO/toluene and monitored by the Kaiser test[66] on growing peptide-resin. The resultant peptide-resin was washed and dried under vacuum. The resin weight gain was determined by gravimetry comparing the starting mass of resin and the final mass of peptide-resin.

Incorporation of Spacer Gly-Gly (2R) or PEG_6 (4R) to 1R. The glycines were subsequently incorporated into the CPP-resin (1200 mg) using the customized protocols and conditions cited above. Fmoc-NH-PEG_6-COOH (2.5 equiv) from Iris Biotech (Germany) was coupled to 150 mg of the peptide-resin using HATU (2.5 equiv) and DIPEA (5 equiv) in DMF (3.5 mL) under microwave irradiation for 2 × 30 min at 60 °C. The progress of each reaction was also monitored by the Kaiser test.[66]

Attachment of 5(6)Carboxyfluorescein (FAM) to 2R and 4R (3R and 5R). FAM, purchased from Sigma-Aldrich, reacted with peptide-resin **2** or **4** also using the following conditions:[39] FAM (5 equiv), BOP (5 equiv), HOBt (5 equiv), DMF (3.5 mL), DIPEA (15 equiv), and 100 mg of **3** or **5** in DMF for 2 × 30 min. The reactions were also assisted by microwaves at 60 °C (5 W). They were also monitored by the Kaiser test.[66]

Incorporation of Chlorin k (Ch_k) into 5R (6R). Ch_k, purchased from Frontier Scientific, reacted with modified peptide-resin **5** under conditions similar to those described above: Ch_k (2.5 equiv), HATU (2.5 equiv), HOBt (2.5 equiv), and 50 mg of **5** in DMF (1.5 mL) for 14.5 h under orbital shaking at 300 rpm and at 60 °C. The reaction progress was monitored by the Kaiser test.[66]

Peptide Detachment from Resin and Simultaneous Full Deprotection. This step was performed suspending 10 mg of the **1R**−**6R** peptide-resin (analytical scale) or 100 mg of **1R**, 2 × 100 mg of **2R**, 2 × 80 mg of **3R**, 90 mg of **4R**, 150 mg of **5R**, and 40 mg of **6R** (preparative scale) in 100 μL (analytical scale) or in 1000 μL of **1R**, **2R**, **3R**, and **4R** or 1500 μL of **5R** or 500 μL (preparative scale) of the mixtures TFA/H_2O/PhOH (95/2.5/2.5; v/v/v) (for **1**−**5**) or TFA/PhOH/H_2O/TIS (88/5/5/2; v/v/v/v) (for **6R**) and keeping the reaction mixture at 60 °C under orbital shaking for 2 h. Then, cold diisopropyl ether (800 μL or 5 mL) was added for peptide precipitation, the resulting suspension was centrifuged, and the

DOI: 10.1021/acsomega.7b01127
ACS Omega 2017, 2, 8156−8166

supernatant was discharged, a procedure repeated three times. Peptide extraction from the solid material was done by adding 800 μL or 3 mL of solutions of 60% ACN/H_2O containing 0.09% TFA, stirring, and centrifugation. The supernatant was then removed, a procedure repeated twice. Finally, the supernatants were pooled and lyophilized to give the crude peptide, which was weighted and characterized.

Purification of Crude Peptides by RP-HPLC. Purifications were performed on a system composed of an automatic gradient controller (Waters 600 Controller), a quaternary pump (Waters Delta 600 Pump), a UV detector (Waters 2487 Dual λ Absorbance), a manual sample injector (Rheodyne 3725i-119), and a register (Kipp & Zonen recorder 124 SE) connected to a preparative C_{18} column (10 μm, 300 Å, 2.2 × 25.0 cm^2, Vydac). The conditions employed are listed in Table S1. The percentages of ACN in solvents B and the linear gradients chosen are related to the nature of the peptides analyzed.

Characterization of Crude and Purified Peptides by RP-HPLC. All analyses were done using a LDC system composed of an automatic gradient controller, two pumps (LDC Analytical, a ConstaMetric 3500 and a ConstaMetric 3200 pump), a UV detector (LDC Analytical spectroMonitor 3100 detector), a manual sample injector (Rheodyne 7125), and an analytical C_{18} column (5 μm, 300 Å, 0.46 × 25 cm^2, Vydac). The software Clarity was used to register the chromatogram obtained. The analytical conditions employed are listed in Table S1.

Characterization of Crude and Purified Products 2−5 by LC-MS. Analyses were performed on an on-line coupling of a RP-HPLC system composed of two pumps (Shimadzu LC-10AD), an analytical C_{18} column (5 μm, 300 Å, 0.46 × 25 cm^2, Vydac), a detector (Shimadzu SDP-10 AV), and an injector coupled to an electrospray (ESI) mass spectrometer with an ion-trap detector (AmaZonX, Bruker Daltonics). The mass spectra were analyzed with the help of HyStar 3.2 software. Analyses employed the same linear gradient and solvent conditions as those used for analytical RP-HPLC.

Amino Acid Analysis. After full hydrolysis of purified peptide conjugates by treatment with HCl 6 mol·L^{-1} at 110 °C for 24 h, amino acid analysis of the hydrolyzate was done using a Dionex BioLC Chromatography system (Sunnyvale/CA) composed by an AS40 automatic sampler, a GS50 quaternary pump, an LC25 column oven, a 2 × 250 mm^2 PA10 AminoPac ion exchange column, and an ED50 electrochemical detector. The amount of each amino acid detected was calculated from comparative analyses using a mixture of 19 amino acids as a standard at known concentrations.

Absorption and Emission Spectra of Free FAM, Ch_k, and Its Conjugates. Solutions (5 μmol·L^{-1}) in 60% ACN/0.09% TFA/water of free FAM, free Ch_k, conjugates **3**, **5**, and **6** were prepared. Samples were put in a cuvette, and absorption spectra (300−800 nm) were recorded with the help of a spectrophotometer (Shimadzu UV-2401PC); however, emission spectra were recorded in a Varian Eclipse Cary fluorescence spectrophotometer. The excitation wavelengths were 492 nm for FAM and conjugates and 410 nm for Ch_k and conjugates.

Evaluation of Ch_k-PEG_6-TAT(47-57)-NH_2 Photosensitizing Properties. Singlet oxygen generation and detection were performed in an especially designed instrument (Edinburgh F900) composed of a laser, cuvette holder, silicon filter, monochromator (liquid-nitrogen-cooled), and a fast multiscaler analyzer card with 5 ns/channel resolution. $^1O_2$ emission spectra were obtained by measuring emission intensities from 1200 to 1350 nm with 1.05 nm steps. Lifetime measurements were performed by accumulation of ∼2000 decays in a time range of 80 μs. Emission spectra were automatically recorded with the help of the instrument software by acquiring decays at various wavelengths, accessing the maximum emission intensity in each wavelength, and plotting the maximum intensity as a function of the wavelength. The solutions of free Ch_k, **4**, and **6** were prepared in a mixture of 60% ACN/H_2O/0.09% TFA and diluted with it directly in the cuvette to have an absorbance of ∼0.10, to be excited at 410 nm. All measurements were performed at room temperature.

Photodegradation of FAM, Ch_k, and Conjugates 3, 5, and 6. Absorption spectra of solutions (10 μmol·L^{-1}) of Ch_k, FAM, and conjugates **3**, **5**, and **6** and pure Ch_k (∼8.5 μmol·L^{-1}) in 60% ACN/H_2O/0.09% TFA were obtained with the help of a spectrophotometer (Shimadzu UV-2401PC) before and after 5 min of laser irradiation (410 nm for Ch_k and conjugate **6**, 440 nm for FAM and conjugates **3** and **5**, pulses of 10 Hz) for 50 min, at room temperature. Then, emission spectra were recorded by plotting the maximum absorbance (at 410 nm for Ch_k and conjugate **6** and at 440 nm for FAM, conjugates, **3** and **5**) as a function of time.

Anticandidal Activity Assay. The antifungal activity was determined by the liquid growth-inhibition method based on the Clinical and Laboratory Standards Institute (CLSI) document M27-A2 and the method described by Bulet.[82] The strains (*Candida parapsilosis*, ATCC 22019) were cultured in Sabouraud Dextrose Agar for 24 h at 35 °C; then, 4−5 colonies from it were collected and incubated in Sabouraud Dextrose Broth at 35 °C overnight and then diluted in fresh broth to have an Abs_{595nm} ∼0.1 and incubated again until the midlogarithmic phase is reached. This inoculum was diluted in Potato Dextrose Broth (Abs_{595nm} = 0.001) to prepare the microplate for the assay. Amphotericin B was used as reference. The microplate prepared was incubated at 35 °C under shaking for 24 h. Peptide concentrations were in the range of 0.19−100 μmol·L^{-1}. The MIC was defined as the lowest concentration that causes total growth inhibition.

Effect of Light Irradiation on the Anticandidal Activity. Because Ch_k is a PS molecule, an extra assay for conjugate 6 was carried out similarly as described above but irradiating the cells with light at 408 nm: after preparing the test plate, it was left in the dark for 30 min to allow conjugate incorporation and then irradiated by a led array (408 nm) for 40 min, to have a total light dose of 10 J·cm^{-2}. Finally, the plate was incubated as described above.

■ ASSOCIATED CONTENT

Supporting Information

The Supporting Information is available free of charge on the ACS Publications website at DOI: 10.1021/acsomega.7b01127.

RP-HPLC conditions employed for analysis and purification of the target compounds and the mass/charge ratios for each compound synthesized, purified, and characterized (**1**−**6** from Scheme 1), in Tables S1 and S2 (PDF)

■ AUTHOR INFORMATION

Corresponding Author

*E-mail: mtmachini@iq.usp.br.

DOI: 10.1021/acsomega.7b01127
ACS Omega 2017, 2, 8156−8166

ORCID
M. Terêsa Machini: 0000-0001-5772-004X

Notes

The authors declare no competing financial interest.

■ ACKNOWLEDGMENTS

M.T.M. is grateful for research support by CNPq (308658/2015-9) and FAPESP (2015/36143-2) grants. C.M.M., Y.M., and M.S.B. acknowledge support by the CNPq/PVE program (400997/2014/2), FAPESP (2015/07508-5; 2013/07937-8), and CNRS/PICS program PhotOxiLip. We thank Thaís Reichert for assistance with the biological assays and Dr. Cleber W. Liria for mass spectrometry and amino acid analyses.

■ ABBREVIATIONS

CPP, cell-penetrating peptide; FAM, 5(6)-carboxyfluorescein; PEG_6, hexaethylene glycol; Ch_k, chlorin k; MIC, minimal inhibitory concentration; PS, photosensitizer; BM, biological membrane; BMM, biomimetic membrane; SPPS, solid-phase peptide synthesis; DFO, desferrioxamine; DFX, deferasirox; Suc, succinic acid; PDT, photodynamic therapy; AMP, antimicrobial peptide; DCM, dicloromethane; DMF, *N*,*N*-dimethylformamide; Fmoc, 9-fluorenylmethoxycarbonyl; HOBt, 1-hydroxybenzotriazole; DIC, *N*,*N*′-diisopropylcarbodiimide; HATU, 1-[bis(dimethylamino)methylene]-1*H*-1,2,3-triazolo[4,5-*b*]pyridinium 3-oxid hexafluorophosphate; DIPEA, *N*,*N*-diipopropylethylamine; BOP, (benzotriazol-1-yloxy) tris-(dimethylamino) phosphonium hexafluorophosphate; TFA, trifluoroacetic acid; Pmc, 2,2,5,7,8-pentamethyl-chroman-6-sulphonyl; RP-HPLC, reverse phase high performance liquid chromatography; LC/ESI-MS, liquid chromatography/electrospray ionization mass spectrometry; ACN, acetonitrile; UV/vis, ultraviolet/visible; Boc, *tert*-butyloxycarbonyl; tBu, *tert*-butyl; DMSO, dimethyl sulfoxide; PhOH, phenol

■ REFERENCES

(1) Di Pisa, M.; Chassaing, G.; Swiecicki, J. M. Translocation Mechanism(s) of Cell-Penetrating Peptides: Biophysical Studies Using Artificial Membrane Bilayers. *Biochemistry* **2015**, *54*, 194−207.
(2) Copolovici, D. M.; Langel, K.; Eriste, E.; Langel, Ü. Cell-Penetrating Peptides: Design, Synthesis, and Applications. *ACS Nano* **2014**, *8*, 1972−1994.
(3) Vivès, E.; Schmidt, J.; Pèlegrin, A. Cell-Penetrating and Cell-Targeting Peptides in Drug Delivery. *Biochim. Biophys. Acta, Rev. Cancer* **2008**, *1786*, 126−138.
(4) Ramsey, J. D.; Flynn, N. H. Cell-Penetrating Peptides Transport Therapeutics into Cells. *Pharmacol. Ther.* **2015**, *154*, 78−86.
(5) Zhang, D.; Wang, J.; Xu, D. Cell-Penetrating Peptides as Noninvasive Transmembrane Vectors for the Development of Novel Multifunctional Drug-Delivery Systems. *J. Controlled Release* **2016**, *229*, 130−139.
(6) Lee, D.; Pacheco, S.; Liu, M. Biological Effects of Tat Cell-Penetrating Peptide: A Multifunctional Trojan Horse? *Nanomedicine* **2014**, *9*, 5−7.
(7) Rudolph, C.; Plank, C.; Lausier, J.; Schillinger, U.; Müller, R. H.; Rosenecker, J. Oligomers of the Arginine-Rich Motif of the HIV-1 TAT Protein Are Capable of Transferring Plasmid DNA into Cells. *J. Biol. Chem.* **2003**, *278*, 11411−11418.
(8) Jafari, M.; Chen, P. Peptide Mediated siRNA Delivery. *Curr. Top. Med. Chem.* **2009**, *9*, 1088−1097.
(9) Mahmood, A.; Prüfert, F.; Efiana, N. A.; Ashraf, M. I.; Hermann, M.; Hussain, S.; Bernkop-Schnürch, A. Cell-Penetrating Self-Nanoemulsifying Drug Delivery Systems (SNEDDS) for Oral Gene Delivery. *Expert Opin. Drug Delivery* **2016**, *13*, 1503−1512.
(10) Marcélis, L.; Kajouj, S.; Ghesquière, J.; Fettweis, G.; Coupienne, I.; Lartia, R.; Surin, M.; Defrancq, E.; Piette, J.; Moucheron, C.; et al. Highly DNA-Photoreactive Ruthenium 1,4,5,8-Tetraazaphenanthrene Complex Conjugated to the TAT Peptide: Efficient Vectorization inside HeLa Cells without Phototoxicity: The Importance of Cellular Distribution. *Eur. J. Inorg. Chem.* **2016**, *2016*, 2902−2911.
(11) Knight, J. C.; Topping, C.; Mosley, M.; Kersemans, V.; Falzone, N.; Fernández-Varea, J. M.; Cornelissen, B. PET Imaging of DNA Damage Using 89Zr-Labelled Anti-gamaH2AX-TAT Immunoconjugates. *Eur. J. Nucl. Med. Mol. Imaging* **2015**, *42*, 1707−1717.
(12) Liu, L.; Dong, X.; Zhu, D.; Song, L.; Zhang, H.; Leng, X. G. TAT-LHRH Conjugated Low Molecular Weight Chitosan as a Gene Carrier Specific for Hepatocellular Carcinoma Cells. *Int. J. Nanomed.* **2014**, *9*, 2879−2889.
(13) Meerovich, I.; Muthukrishnan, N.; Johnson, G. A.; Erazo-Oliveras, A.; Pellois, J. P. Photodamage of Lipid Bilayers by Irradiation of a Fluorescently Labeled Cell-Penetrating Peptide. *Biochim. Biophys. Acta, Gen. Subj.* **2014**, *1840*, 507−515.
(14) Hudecz, F.; Bánóczi, Z.; Csík, G. Medium-Sized Peptides as Built in Carriers for Biologically Active Compounds. *Med. Res. Rev.* **2005**, *25*, 679−736.
(15) Mecke, A.; Dittrich, C.; Meier, W. Biomimetic Membranes Designed from Amphiphilic Block Copolymers. *Soft Matter* **2006**, *2*, 751−759.
(16) Deniaud, A.; Rossi, C.; Berquand, A.; Homand, J.; Campagna, S.; Knoll, W.; Brenner, C.; Chopineau, J. Voltage-Dependent Anion Channel Transports Calcium Ions through Biomimetic Membranes. *Langmuir* **2007**, *23*, 3898−3905.
(17) Makky, A.; Tanaka, M. Impact of Lipid Oxidization on Biophysical Properties of Model Cell Membranes. *J. Phys. Chem. B* **2015**, *119*, 5857−5863.
(18) Dennison, S. R.; Baker, R. D.; Nicholl, I. D.; Phoenix, D. A. Interactions of Cell Penetrating Peptide Tat with Model Membranes: A Biophysical Study. *Biochem. Biophys. Res. Commun.* **2007**, *363*, 178−182.
(19) Wang, F.; Wang, Y.; Zhang, X.; Zhang, W.; Guo, S.; Jin, F. Recent Progress of Cell-Penetrating Peptides as New Carriers for Intracellular Cargo Delivery. *J. Controlled Release* **2014**, *174*, 126−136.
(20) Silhol, M.; Tyagi, M.; Giacca, M.; Lebleu, B.; Vivès, E. Different Mechanisms for Cellular Internalization of the HIV-1 Tat-Derived Cell Penetrating Peptide and Recombinant Proteins Fused to Tat. *Eur. J. Biochem.* **2002**, *269*, 494−501.
(21) Brooks, H.; Lebleu, B.; Vivès, E. Tat Peptide-Mediated Cellular Delivery: Back to Basics. *Adv. Drug Delivery Rev.* **2005**, *57*, 559−577.
(22) Srinivasan, D.; Muthukrishnan, N.; Johnson, G. A.; Erazo-Oliveras, A.; Lim, J.; Simanek, E. E.; Pellois, J. P. Conjugation to the Cell-Penetrating Peptide TAT Potentiates the Photodynamic Effect of Carboxytetramethylrhodamine. *PLoS One* **2011**, *6*, No. e17732.
(23) Goswami, D.; Vitorino, H. A.; Alta, R. Y. P.; Silvestre, D. M.; Nomura, C. S.; Machini, M. T.; Espósito, B. P. Deferasirox-TAT(47-57) Peptide Conjugate as a Water Soluble, Bifunctional Iron Chelator with Potential Use in Neuromedicine. *BioMetals* **2015**, *28*, 869−877.
(24) Fosgerau, K.; Hoffmann, T. Peptide Therapeutics: Current Status and Future Directions. *Drug Discovery Today* **2015**, *20*, 122−128.
(25) Lau, J. L.; Dunn, M. K. Therapeutic Peptides: Historical Perspectives, Current Development Trends, and Future Directions *Bioorg. Med. Chem.* 2017. 10.1016/j.bmc.2017.06.052.
(26) Vivès, E.; Brodin, P.; Lebleu, B. A Truncated HIV-1 Tat Protein Basic Domain Rapidly Translocates through the Plasma Membrane and Accumulates in the Cell Nucleus. *J. Biol. Chem.* **1997**, *272*, 16010−16017.
(27) Grunwald, J.; Rejtar, T.; Sawant, R.; Wang, Z.; Torchilin, V. P. TAT Peptide and Its Conjugates: Proteolytic Stability. *Bioconjugate Chem.* **2009**, *20*, 1531−1537.
(28) Hu, M.; Chen, P.; Wang, J.; Chan, C.; Scollard, D. A.; Reilly, R. M. Site-Specific Conjugation of HIV-1 Tat Peptides to IgG: A Potential Route to Construct Radioimmunoconjugates for Targeting

DOI: 10.1021/acsomega.7b01127
ACS Omega 2017, 2, 8156−8166

Intracellular and Nuclear Epitopes in Cancer. *Eur. J. Nucl. Med. Mol. Imaging* **2006**, *33*, 301−310.
(29) Kale, A. A.; Torchilin, V. P. Enhanced Transfection of Tumor Cells in Vivo using "Smart" pH-Sensitive TAT-Modified Pegylated Liposomes. *J. Drug Targeting* **2007**, *15*, 538−545.
(30) Song, J.; Zhang, Y.; Zhang, W.; Chen, J.; Yang, X.; Ma, P.; Zhang, B.; Liu, B.; Ni, J.; Wang, R. Cell Penetrating Peptide TAT Can Kill Cancer Cells via Membrane Disruption after Attachment of Camptothecin. *Peptides* **2015**, *63*, 143−149.
(31) Sibrian-Vazquez, M.; Hao, E.; Jensen, T. J.; Vicente, M. G. H. Enhanced Cellular Uptake with a Cobaltacarborane − Porphyrin − HIV-1 Tat 48 − 60 Conjugate. *Bioconjugate Chem.* **2006**, *17*, 928−934.
(32) Sibrian-Vazquez, M.; Jensen, T. J.; Hammer, R. P.; Vicente, M. G. H. Peptide-Mediated Cell Transport of Water Soluble Porphyrin Conjugates. *J. Med. Chem.* **2006**, *49*, 1364−1372.
(33) Goswami, D.; Machini, M. T.; Silvestre, D. M.; Nomura, C. S.; Espósito, B. P. Cell Penetrating Peptide (CPP)-Conjugated Desferrioxamine for Enhanced Neuroprotection: Synthesis and in Vitro Evaluation. *Bioconjugate Chem.* **2014**, *25*, 2067−2080.
(34) Alta, R. Y. P.; Vitorino, H. A.; Goswami, D.; Liria, C. W.; Wisnovsky, S. P.; Kelley, S. O.; Machini, M. T.; Espósito, B. P. Mitochondria-Penetrating Peptides Conjugated to Desferrioxamine as Chelators for Mitochondrial Labile Iron. *PLoS One* **2017**, *12*, No. e0171729.
(35) Sabnis, R. W. *Handbook of Fluorescent Dyes and Probes*; John Wiley & Sons, Inc.: Hoboken, New Jersey, 2015; pp110−118.
(36) Kvach, M. V.; Tsybulsky, D. A.; Ustinov, A. V.; Stepanova, I. A.; Bondarev, S. L.; Gontarev, S. V.; Korshun, V. A.; Shmanai, V. V. 5(6)-Carboxyfluorescein Revisited: New Protecting Group, Separation of Isomers, and Their Spectral Properties on Oligonucleotides. *Bioconjugate Chem.* **2007**, *18*, 1691−1696.
(37) Ueno, Y.; Jiao, G. S.; Burgess, K. Preparation of 5- and 6-Carboxyfluorescein. *Synthesis* **2004**, 2591−2593.
(38) Onoue, S.; Liu, B.; Nemoto, Y.; Hirose, M.; Yajima, T. Chemical Synthesis and Application of C-Terminally 5-Carboxyfluorescein-Labelled Thymopentin as a Fluorescent Probe for Thymopoietin Receptor. *Anal. Sci.* **2006**, *22*, 1531−1535.
(39) Remuzgo, C.; Oewel, T. S.; Daffre, S.; Lopes, T. R. S.; Dyszy, F. H.; Schreier, S.; Machado-Santelli, G. M.; Terêsa Machini, M. Chemical Synthesis, Structure-Activity Relationship, and Properties of Shepherin I: A Fungicidal Peptide Enriched in Glycine-Glycine-Histidine Motifs. *Amino Acids* **2014**, *46*, 2573−2586.
(40) Li, S. Y.; Cheng, H.; Xie, B. R.; Qiu, W. X.; Song, L. L.; Zhuo, R. X.; Zhang, X. Z. A Ratiometric Theranostic Probe for Tumor Targeting Therapy and Self-Therapeutic Monitoring. *Biomaterials* **2016**, *104*, 297−309.
(41) Pandey, S. K.; Kaur, J.; Easwaramoorthy, B.; Shah, A.; Coleman, R.; Mukherjee, J. Multimodality Imaging Probe for Positron Emission Tomography and Fluorescence Imaging Studies. *Mol. Imaging* **2014**, *13*, 1−8.
(42) Carvalho, L. A. C.; Remuzgo, C.; Perez, K. R.; Machini, M. T. Hb40-61a: Novel Analogues Help Expanding the Knowledge on Chemistry, Properties and Candidacidal Action of This Bovine Alfa-Hemoglobin-Derived Peptide. *Biochim. Biophys. Acta, Biomembr.* **2015**, *1848*, 3140−3149.
(43) Eggimann, G.A.; Buschor, S.; Darbre, T.; Reymond, J.-L. Convergent Synthesis and Cellular Uptake of Multivalent Cell Penetrating Peptides Derived from Tat, Antp, pVEC, TP10 and SAP. *Org. Biomol. Chem.* **2013**, *11*, 6717−6733.
(44) Henriques, S. T.; Castanho, M. A. R. B. Environmental Factors That Enhance the Action of the Cell Penetrating Peptide Pep-1: A Spectroscopic Study Using Lipidic Vesicles. *Biochim. Biophys. Acta, Biomembr.* **2005**, *1669*, 75−86.
(45) Thorén, P. E. G.; Persson, D.; Esbjörner, E. K.; Goksör, M.; Lincoln, P.; Nordén, B. Membrane Binding and Translocation of Cell-Penetrating Peptides. *Biochemistry* **2004**, *43*, 3471−3489.
(46) Abrahamse, H.; Hamblin, M. R. New Photosensitizers for Photodynamic Therapy. *Biochem. J.* **2016**, *473*, 347−364.
(47) Foote, C. S. Mechanisms of Photosensitized Oxidation. *Science* **1968**, *162*, 963−970.
(48) Oliveira, C. S.; Turchiello, R.; Kowaltowski, A. J.; Indig, G. L.; Baptista, M. S. Major Determinants of Photoinduced Cell Death: Subcellular Localization versus Photosensitization Efficiency. *Free Radical Biol. Med.* **2011**, *51*, 824−833.
(49) Dougherty, T. J.; Gomer, C. J.; Henderson, B. W.; Peng, Q.; et al. Photodynamic Therapy. *JNCI, J. Natl. Cancer Inst.* **1998**, *90*, 889−905.
(50) Schneider, R.; Tirand, L.; Frochot, C.; Vanderesse, R.; Thomas, N.; Gravier, J.; Guillemin, F.; Barberi-Heyob, M. Recent Improvements in the Use of Synthetic Peptides for a Selective Photodynamic Therapy. *Anti-Cancer Agents Med. Chem.* **2006**, *6*, 469−488.
(51) Boylet, R. W.; Dolphin, D. Structure and Biodistribution Relationships of Photodynamic Sensitizers. *Photochem. Photobiol.* **1996**, *64*, 469−485.
(52) Sibani, S. A.; McCarron, P. A.; Woolfson, A. D.; Donnelly, R. F. Photosensitiser Delivery for Photodynamic Therapy. Part 2: Systemic Carrier Platforms. *Expert Opin. Drug Delivery* **2008**, *5*, 1241−1254.
(53) Hamblin, M. R.; Newman, E. L. Photosensitizer Targeting in Photodynamic Therapy I. Conjugates of Haematoporphyrin with Albumin and Transferrin. *J. Photochem. Photobiol., B* **1994**, *26*, 45−56.
(54) van Dongen, G. A. M. S.; Visser, G. W. M.; Vrouenraets, M. B. Photosensitizer-Antibody Conjugates for Detection and Therapy of Cancer. *Adv. Drug Delivery Rev.* **2004**, *56*, 31−52.
(55) He, F.; Ren, X.; Shen, X.; Xu, Q. H. Water-Soluble Conjugated Polymers for Amplification of One- and Two-Photon Properties of Photosensitizers. *Macromolecules* **2011**, *44*, 5373−5380.
(56) Ohtsuki, T.; Miki, S.; Kobayashi, S.; Haraguchi, T.; Nakata, E.; Hirakawa, K.; Sumita, K.; Watanabe, K.; Okazaki, S. The Molecular Mechanism of Photochemical Internalization of Cell Penetrating Peptide-Cargo-Photosensitizer Conjugates. *Sci. Rep.* **2015**, *5*, No. 18577.
(57) Sehgal, I.; Sibrian-Vazquez, M.; Vicente, M. G. H. Photoinduced Cytotoxicity and Biodistribution of Prostate Cancer Cell-Targeted Porphyrins. *J. Med. Chem.* **2008**, *51*, 6014−6020.
(58) New, O. M.; Dolphin, D. Design and Synthesis of Novel Phenothiazinium Photosensitiser Derivatives. *Eur. J. Org. Chem.* **2009**, 2675−2686.
(59) Veronese, F. M. Peptide and Protein PEGylation: A Review of Problems and Solutions. *Biomaterials* **2001**, *22*, 405−417.
(60) Bechinger, B.; Goor, S.-U. Antimicrobial Peptides: Mechanisms of Action and Resistance. *J. Dent. Res.* **2017**, *96*, 254−260.
(61) Dosselli, R.; Tampieri, C.; Ruiz-González, R.; De Munari, S.; Ragàs, X.; Sánchez-García, D.; Agut, M.; Nonell, S.; Reddi, E.; Gobbo, M. Synthesis, Characterization, and Photoinduced Antibacterial Activity of Porphyrin-Type Photosensitizers Conjugated to the Antimicrobial Peptide Apidaecin 1b. *J. Med. Chem.* **2013**, *56*, 1052−1063.
(62) Loffredo, C.; Assunção, N. A.; Gerhardt, J.; Miranda, M. T. M. Microwave-Assisted Solid-Phase Peptide Synthesis at 60 Degrees C: Alternative Conditions with Low Enantiomerization. *J. Pept. Sci.* **2009**, *15*, 808−817.
(63) Remuzgo, C.; Andrade, G. F. S.; Temperini, M. L. A.; Miranda, M. T. M. Acanthoscurrin Fragment 101−132: Total Synthesis at 60 °C of a Novel Difficult Sequence. *Biopolymers* **2009**, *92*, 65−75.
(64) Ramesh, S.; Torre, B. G. De; Albericio, F.; Kruger, H. G.; Govender, T. Microwave-Assisted Synthesis of Antimicrobial Peptides. In *Antimicrobial Peptides*; Springer, 2017; Vol. *1548*, pp 51−59.
(65) Pratesi, A.; Stazzoni, S.; Lumini, M.; Sabatino, G.; Carotenuto, A.; Brancaccio, D.; Novellino, E.; Chinol, M.; Rovero, P.; Ginanneschi, M.; et al. Synthesis of Dicarba-Cyclooctapeptide Somatostatin Analogs by Conventional and MW-Assisted RCM: A Study about the Impact of the Configuration at C α of Selected Amino Acids. *Chem. Eng. Process.* **2017**, 1−8.
(66) Kaiser, E.; Colescott, R. L.; Bossinger, C. D.; Cook, P. I. Color Test for Detection of Free Terminal Amino Groups in the Solid-Phase Synthesis of Peptides. *Anal. Biochem.* **1970**, *34*, 595−598.

DOI: 10.1021/acsomega.7b01127
ACS Omega 2017, 2, 8156−8166

(67) Bodanszky, M.; Deshmane, S. S.; Martinez, J. Side Reactions in Peptide Synthesis. 11. Possible Removal of the 9-Fluorenylmethyloxycarbonyl Group by the Amino Components during Coupling. *J. Org. Chem.* **1979**, *44*, 1622−1625.
(68) Jamous, M.; Tamma, M. L.; Gourni, E.; Waser, B.; Reubi, J. C.; Maecke, H. R.; Mansi, R. PEG Spacers of Different Length Influence the Biological Profile of Bombesin-Based Radiolabeled Antagonists. *Nucl. Med. Biol.* **2014**, *41*, 464−470.
(69) Carpino, L. A.; El-Faham, A.; Minor, C. A.; Albericio, F. Advantageous Applications of Azabenzotriazole (Triazolopyridine)-Based Coupling Reagents to Solid-Phase Peptide Synthesis. *J. Chem. Soc., Chem. Commun.* **1994**, 201−203.
(70) Choi, Y.; McCarthy, J. R.; Weissleder, R.; Tung, C. H. Conjugation of a Photosensitizer to an Oligoarginine-Based Cell-Penetrating Peptide Increases the Efficacy of Photodynamic Therapy. *ChemMedChem* **2006**, *1*, 458−463.
(71) Pescina, S.; Sala, M.; Padula, C.; Scala, M. C.; Spensiero, A.; Belletti, S.; Gatti, R.; Novellino, E.; Campiglia, P.; Santi, P.; et al. Design and Synthesis of New Cell Penetrating Peptides: Diffusion and Distribution inside the Cornea. *Mol. Pharmaceutics* **2016**, *13*, 3876−3883.
(72) Cerrato, C. P.; Pirisinu, M.; Vlachos, E. N.; Langel, Ü. Novel Cell-Penetrating Peptide Targeting Mitochondria. *FASEB J.* **2015**, *29*, 4589−4599.
(73) Angeles-Boza, A. M.; Erazo-Oliveras, A.; Lee, Y. J.; Pellois, J. P. Generation of Endosomolytic Reagents by Branching of Cell-Penetrating Peptides: Tools for the Delivery of Bioactive Compounds to Live Cells in Cis or Trans. *Bioconjugate Chem.* **2010**, *21*, 2164−2167.
(74) Wilkinson, F.; et al. Rate Constants for the Decay and Reactions of the Lowest Electronically Excited Singlet State of Molecular Oxygen in Solution. *J. Phys. Chem. Ref. Data* **1995**, *24*, 663−1021.
(75) Jung, H. J.; Park, Y.; Hahm, K. S.; Lee, D. G. Biological Activity of Tat (47-58) Peptide on Human Pathogenic Fungi. *Biochem. Biophys. Res. Commun.* **2006**, *345*, 222−228.
(76) Jung, H. J.; Jeong, K. S.; Lee, D. G. Effective Antibacterial Action of Tat (47-58) by Increased Uptake into Bacterial Cells in the Presence of Trypsin. *J. Microbiol. Biotechnol.* **2008**, *18*, 990−996.
(77) Tosun, I.; Akyuz, Z.; Guler, N. C.; Gulmez, D.; Bayramoglu, G.; Kaklikkaya, N.; Arikan-Akdagli, S.; Aydin, F. Distribution, Virulence Attributes and Antifungal Susceptibility Patterns of *Candida parapsilosis* Complex Strains Isolated from Clinical Samples. *Med. Mycol.* **2013**, *51*, 483−492.
(78) Holm, T.; Bruchmann, J.; Scheynius, A.; Langel, Ü. Cell-Penetrating Peptides as Antifungals towards Malassezia Sympodialis. *Lett. Appl. Microbiol.* **2012**, *54*, 39−44.
(79) Yan, H.; Hancock, R. E. W. Synergistic Interactions between Mammalian Antimicrobial Defense Peptides. *Antimicrob. Agents Chemother.* **2001**, *45*, 1558−1560.
(80) Splith, K.; Neundorf, I. Antimicrobial Peptides with Cell-Penetrating Peptide Properties and Vice Versa. *Eur. Biophys. J.* **2011**, *40*, 387−397.
(81) Varanda, L. M.; Miranda, M. T. Solid-Phase Peptide Synthesis at Elevated Temperatures: A Search for and Optimized Synthesis Condition of Unsulfated Cholecystokinin-12. *J. Pept. Res.* **1997**, *50*, 102−108.
(82) Bulet, P.; Dimarcq, J. L.; Hetru, C.; Lagueux, M.; Charlet, M.; Hegy, G.; Van Dorsselaer, A.; Hoffmann, J. A. A Novel Inducible Antibacterial Peptide of Drosophila Carries an O-Glycosylated Substitution. *J. Biol. Chem.* **1993**, *268*, 14893−14897.

DOI: 10.1021/acsomega.7b01127
ACS Omega 2017, 2, 8156−8166